European Journal of Medical Research

RESEARCH

Open Access

Alcohol promotes CPT1A-induced lipid metabolism disorder to sentinel-regulate acute pancreatitis

Zenghui Li[1†], Xinghui Li[1†], Hui Jiang[2†], Jingdong Li[3], Bin Xiao[4], Yong Chen[5], Shunhai Jian[6], Mei Zeng[7*] and Xiaoming Zhang[1*]

Abstract

Background and aims Previous studies have confirmed that alcohol can increase the sensitivity of the pancreas to stressors and exacerbate the severity of pancreatitis when excessive alcohol intake is combined with other causes. In the current work, this study attempted to explore how does alcohol regulate cerulein-induced acute pancreatitis, especially before inflammation occurs.

Methods Proteomics was performed to analyze the differentially expressed proteins in pancreatic tissues from a rat model of pancreatitis. The metabolite levels in the pancreatic tissue, serum of rats and serum of persons with a history of alcohol consumption were detected by LC–MS/MS. In the present study the impact of etomoxir (a carnitine palmitoyl-transferase 1A-specific inhibitor) treatment on AR42J cells treated with alcohol and the effect of etomoxir injection on the inflammatory response in an alcohol + cerulein-induced AAP rat model was evaluated.

Results When treated with the same amount of cerulein, the rats that ingested alcohol presented with more severe pancreatitis. The proteomics results revealed that the fatty acid degradation pathway was closely related to the development of alcoholic acute pancreatitis, and CPT1A exhibited the greatest increase (approximately twofold increase). The products (acylcarnitines) of CPT1A were changed in the serum of persons with a history of alcohol consumption. Etomoxir treatment mitigates the influence of alcohol stimulation on the aberrant expression of proteins associated with oxidative stress, increased ROS production, mitochondrial ultrastructural alterations and mitochondrial dysfunction in AR42J cells. Etomoxir injection reduced the inflammatory response in the AAP rat model.

Conclusion Alcohol upregulates CPT1A protein expression in pancreatic tissue, resulting in abnormal lipid metabolism. The products of lipid metabolism, ROS, contribute to mitochondrial ultrastructural alterations and mitochondrial dysfunction. These changes act as sentinel events that regulate acute pancreatitis.

Keywords Acute pancreatitis, Proteomics, Mitochondrial dysfunction, Lipid metabolism

†Zenghui Li, Xinghui Li and Hui Jiang contributed equally to this work.

*Correspondence:
Mei Zeng
zengmei123@nsmc.edu.cn
Xiaoming Zhang
cjr.zhxm@vip.163.com
Full list of author information is available at the end of the article

Introduction

The common contributing factors of acute pancreatitis (AP) are gallstones and alcohol consumption, which account for approximately 40% and 30% of cases, respectively [1]. Patients with a long history of alcohol consumption tend to develop severe AP rather than mild AP [2]. Compared with cerulein-induced AP, alcohol-pretreated AP leads to a more severe inflammatory response. A previous study revealed that alcohol, along with its metabolites, results in mutual contact between lysosomal and digestive enzymes and exacerbates the vulnerability of pancreatic organelles. Furthermore, these alterations lead to premature intracellular activation of trypsinogen, and the gland is susceptible to autodigestive injury and necroinflammation after being exposed to triggering factors [3].

Growing evidence indicates that alcohol leads to loss of mitochondrial membrane potential (MMP) and eventually to adenosine triphosphate depletion, and in this context, the exposed pancreas is prone to necrosis and pancreatitis [4]. This effect may be mediated through oxidative alcohol metabolism, in which alcohol dehydrogenase (ADH) oxidizes alcohol to acetaldehyde, which is subsequently chemically converted to acetic acid by aldehyde dehydrogenase isoenzyme 2 (ALDH2), which is located exclusively in the mitochondria. Shalbueva et al. reported that the loss of MMP is mediated by mitochondrial permeability transition pore (MPTP) activation resulting from oxidative alcohol metabolism [4]. Notably, oxidative alcohol metabolism occurs primarily in the liver. The pancreas metabolizes alcohol primarily through fatty acid ethyl ester (FAEE) synthase, which produces FAEEs and is involved in nonoxidative alcohol metabolism [5, 6]. Both oxidative alcohol metabolism and nonoxidative alcohol metabolism lead to a decrease in NAD^+, resulting in MMP depolarization. Interestingly, several studies have shown that reactive oxygen species (ROS), intermediate products of redox reactions in aerobic metabolism [7], induce mitochondrial damage and loss of membrane potential, resulting in mitochondrial dysfunction [8, 9]. However, the relationship between alcohol consumption and ROS production in the mitochondria of pancreatic tissue in AAP has not been investigated.

In the present study, alcohol was hypothesized to disorder lipid metabolism and promote ROS production in the mitochondria of pancreatic tissues, which act as sentinel events to regulate acute pancreatitis. This study provides initial evidence that the suppression of lipid metabolism-induced ROS production has therapeutic effects on AAP through the alleviation of mitochondrial dysfunction.

Materials and methods

Animals

Male Sprague–Dawley rats (200–250 g, purchased from North Sichuan Medical College, Sichuan, China) were maintained in a room at a temperature of 22 ± 1 °C with a light/dark cycle of 12 h. The rats were fasted for 24 h prior to the experiment but were allowed to drink freely.

Induction of AAP and sample preparation

Commercially available liquid food (Lieber-DeCarli [10], consisting of 36 kcal% alcohol calories; HD010; Biotech Co. Ltd., Beijing, China) was fed to 6-week-old rats ($n = 10$) in the alcohol + cerulein (HY-A0190, MCE, NJ, USA)-treated group (experimental group 3) and alcohol-treated group (experimental group 1) for 14 weeks to establish an alcohol-fed model as described previously [11]. In the cerulein-treated group (experimental group 2) and control group, 6-week-old rats ($n = 10$) were fed an isocaloric control diet for 14 weeks. The cerulein-treated group ($n = 5$) and the alcohol + cerulein-treated group ($n = 5$) received 3 hypodermics injections of cerulein (50 μg) or vehicle (0.9% NaCl) per kilogram of body weight, hourly, according to the previously study [12]. The animals were anesthetized with isoflurane two hours after the last injection, blood was harvested by cardiac puncture, and thereafter, the animals were euthanized. The supernatants were collected after the samples were centrifuged and then stored in a − 80 °C freezer for subsequent analysis. Pancreatic tissue was quickly separated from the surrounding lymph nodes and adipose tissue for the experiments, and islet tissue was also removed. A small portion of pancreatic tissue was fixed in 4% formalin for HE and immunofluorescence assays. The remaining pancreatic tissue was stored in a − 80 °C freezer for proteomics analysis.

Description of experimental group

Experimental group 1: alcohol-treated only to establish an alcohol-fed model, not to induce acute pancreatitis; experimental group 2: treated with 3 hypodermics injections of cerulein to induce acute pancreatitis; experimental group 3: treated with alcohol-fed and 3 hypodermics injections of cerulein to induce alcoholic acute pancreatitis.

Lipidomics analysis

Briefly, samples were first spiked with an appropriate amount of internal lipid standards and then homogenized with 200 μL of water and 240 μL of methanol. After that, 800 μL of MTBE was added, and the mixture

was ultrasonicated for 20 min at 4 °C, followed by incubation for 30 min at room temperature. The solution was centrifuged at 14,000×*g* for 15 min at 10 °C, and the upper organic solvent layer was obtained and dried under nitrogen. Reversed-phase chromatography was selected for LC separation using a CSH C18 column (1.7 μm, 2.1 mm × 100 mm, Waters). The lipid extracts were redissolved in 200 μL of 90% isopropanol/acetonitrile and centrifuged at 14,000×*g* for 15 min. Finally, 3 μL of sample was injected. Solvent A was acetonitrile–water (6:4, v/v) with 0.1% formic acid and 0.1 mM ammonium formate, and solvent B was acetonitrile–isopropanol (1:9, v/v) with 0.1% formic acid and 0.1 mM ammonium formate. The initial mobile phase was 30% solvent B at a flow rate of 300 μL/min and, was held for 2 min, then linearly increased to 100% solvent B at 23 min, and maintained at 5% solvent B for 10 min. Mass spectra were acquired by Q Exactive Plus in positive and negative mode, respectively.

ELISA

Serum levels of IL-1β, TNFα, IL-8 and IL-6 were determined by ELISA kits according to the manufacturer's instructions (IL-1β: D731007, Sangon Biotech Co., Ltd., Shanghai, China; TNFα: d731168, Sangon Biotech Co., Ltd., Shanghai, China; IL-8: SKER-0071, Beijing Solarbio Science & Technology Co., Ltd.; IL-6: D731010, Sangon Biotech Co., Ltd., Shanghai, China).

Cell experiments

The AR42J, bought from ATCC, were cultured in RPMI-1640 medium containing 10% FBS. Then, upon attaining a 60% confluence, they were incubated under synchronized conditions for 24 h before being grouped. Then, it was incubated with the following parameters: 5% CO_2 at 37 °C, subsequently digested with 0.25% trypsin, and cultured for 7 days. The cells were seeded in 25-cm^2 culture flasks with density of 1 × 105 cells/mL. Alcohol at various concentrations (2.5, 5 and 10 μg/mL) was applied for 8 h to stimulate the AR42J cells.

Detection of amylase activity

Serum amylase activity was measured with an enzyme colorimetric assay kit (Roche Diagnostics, Indianapolis, IN). Amylase activity in the supernatant of cells and culture medium was determined by using an iodine–starch colorimetric kit from Jiancheng Bioengineering Institute (C016-1-1, Nanjing, China) following the manufacturer's instructions.

HE staining and scoring

Sections of paraffin-embedded tissues were sectioned and stained with hematoxylin–eosin (HE). A minimum of 10 fields of view (entire sample area: 4 mm^2) were randomly chosen for each section and scored as follows: 0 = none, 1 = mild (< 10% of field of view), 2 = moderate (10%–50% of field of view), and 3 = severe (> 50% of field of view).

Determination of mitochondrial and total ROS

Mitochondrial and cellular ROS levels were determined with the MitoSOX fluorescence probe (MCE, NJ, USA) and the DCFH-DA fluorescence probe (MCE, NJ, USA), respectively, through flow cytometry (FACS) in accordance with the manufacturer's instructions. The mean fluorescence intensity (MFI) of PE-Texas Red-H was quantified with FlowJo software.

MMP detection

The MMP was assessed via a JC-1 probe (Beyotime, Shanghai, China, 2006) according to the manufacturer's instructions. In brief, PECs were stained utilizing a JC-1 probe and later assayed via FACS or Olympus laser confocal microscope imaging analysis. FlowJo software utilizes the PE-H (MFI)/FITC-H (MFI) ratio to represent alterations in the MMP for FACS analysis.

Inhibition of CPT1A activity in the rat model of AAP

In the alcohol + cerulein + etomoxir-treated group and alcohol + cerulein-treated group, 6-week-old rats ($n = 10$) were fed a commercially available liquid diet (Lieber-DeCarli [10] with 36 kcal% alcohol calories; HD010; Biotech Co. Ltd., Beijing, China) for 13 weeks. Beginning in the 14th week, the alcohol + cerulein + etomoxir-treated group ($n = 5$) received intraperitoneal injections of vehicle (0.9% NaCl) or etomoxir (CAS No. 124083-20-1, Med Chem Express, NJ, USA) (with a body weight of 20 mg/kg) for 7 d, according to the MCE official website [13]. Beginning in the 15th week, the alcohol + cerulein + etomoxir-treated group and alcohol + cerulein-treated group ($n = 5$) received 3 hypodermics injections of vehicle (0.9% NaCl) or cerulein (50 μg) per kilogram of body weight, hourly. The animals were anesthetized with isoflurane two hours after the last injection, blood was harvested by cardiac puncture, and thereafter, the animals were euthanized. The specimens were preserved as described above.

Clinical data

The analysis was based on the metabolomics data of 40 participants (participants information is in Table 1): 20 persons with a history of alcohol consumption (PHA) and without other diseases (including abnormal liver function, severe alcoholism or adverse symptoms of acute pancreatitis) and 20 healthy individuals with no drinking history. Acylcarnitines in serum samples were determined semiquantitatively by liquid

Table 1 Participants information

	PHA ($n=20$)	Control ($n=20$)	*P* value
Male (%)	19 (95%)	10 (50%)	0.000
Age (years)	46.87 ± 11.35	51.98 ± 16.40	0.028
Race (Han nationality)	20	20	–
Drinking level (g)	19 ± 5.08	0	0.000

PHA persons with a history of alcohol consumption

chromatography–tandem mass spectrometry. Ethical approval to perform this study was obtained from the Institutional Review Board (IRB), and informed consent was waived.

Statistical analysis

Differences between both groups of animals were examined with Student's *t* test. ANOVA was conducted, and multiple comparisons were performed utilizing the LSD test to assess the significance of differences between multiple groups of animals (IBM SPSS Statistics for Windows, v.26, IBM Crop., Armonk, NY). Differences were regarded as statistically significant when the *P* value was less than 0.05.

*For details on the proteomics analysis, detection of acylcarnitines in serum samples, detection of acylcarnitines, western blotting, immunofluorescence staining, analysis of mitochondrial function [14], and examination via electron microscopy, please see Materials and methods in Supplementary Information.

Results

Alcohol treatment aggravates cerulein-induced AP in rats

The serum amylase data for the four groups of model rats showed that the serum amylase activity of the cerulein-induced AP model rats and alcohol + cerulein-induced AAP model rats was evidently greater than that of the control group rats, and alcohol treatment alone had no significant effect on amylase activity (Fig. 1A). Histological analysis revealed more severe damage to the pancreas in the AAP model rats than in the AP model rats. However, alcohol treatment alone had little effect on the pathological score (Fig. 1B). The immunofluorescence results showed increased infiltration of neutrophils (Ly6G- and MPO-positive cells) in the pancreas of AAP model rats compared to that in the pancreas of AP model rats, but only alcohol-treated rats showed almost no neutrophil infiltration (Fig. 1C). Significant evidence from a previous study [15] has shown that TNFα acts in the pathogenesis of AP. The serum TNFα level was markedly greater in the AAP and AP model rats than in the control group. In contrast to that in the AP model rats, the serum TNFα level in the AAP model rats increased to a greater extent (Fig. 1D). The level of serum TNFα in the alcohol-treated rats was almost the same as that in the control group. The serum IL-8, IL-6 and IL-1β levels did not significantly change among the four groups of rats. These data suggest that alcohol pretreatment exacerbates cerulein-induced AP in rats.

Alcohol treatment markedly enhances CPT1A expression in rat pancreatic tissues

To investigate the molecular mechanisms by which alcohol exacerbates inflammation in AP rats, protein expression profiles were characterized in pancreatic tissue from control rats, alcohol-treated rats, AP model rats, and AAP model rats by performing quantitative proteomics based on tandem mass tag (TMT) analysis. In the present study, differentially expressed proteins (DEPs; fold change > 1.2 or < 0.8; $P<0.05$) of organelle localization were identified in pancreatic tissue from AAP model rats versus AP model rats: 115 DEPs were located in the nucleus, 101 DEPs were located in the extracellular space, 84 DEPs were located in the cytoplasm, 73 DEPs were located in mitochondria, 53 DEPs were located in the plasma membrane and 10 DEPs were located in chloroplasts. KEGG analysis revealed enrichment of proteins related to the fatty acid degradation pathway (Fig. 2A). Volcano plots revealed 242 DEPs, of which 165 were upregulated (based on a cutoff value of 1.2-fold) and 77 were downregulated (based on a cutoff value of 0.8-fold). Fatty acid degradation is mainly carried out on mitochondria. Therefore, this study targeted DEPs that were located in mitochondria and related to the fatty acid degradation pathway, and the expression of 12 DEPs was upregulated (Fig. 2B). Among these DEPs, CPT1A was shown to have the most significantly upregulated expression, which was approximately twofold greater (Fig. 2C). However, the protein levels of CPT1A were not significantly different in the pancreatic tissue of alcohol-treated rats compared with those in the pancreatic tissue of AAP model rats or AP model rats versus control rats. Moreover, proteomics revealed that the protein expression of HADH, HADHA, HADHB, ACADL, ACADVL, ACADS, ACADM, ACAT1, ECI1, CPT2, ACAA2 and ACSL3, which are related to the processes of fatty acid oxidation (FAO) and lipid metabolism, was upregulated. For a full list of these abbreviations, see the Supplemental and Materials in Supplementary Information. Considering the proteomics analysis, this study mapped the related key proteins that exhibited altered expression patterns in the pancreatic tissue of AAP model rats (Fig. 3). CPT1A is a rate-limiting enzyme [16] that mediates FAO, and this research was particularly interested in this enzyme. Consistent with the proteomic data, the immunofluorescence (IF) results revealed a clear increase

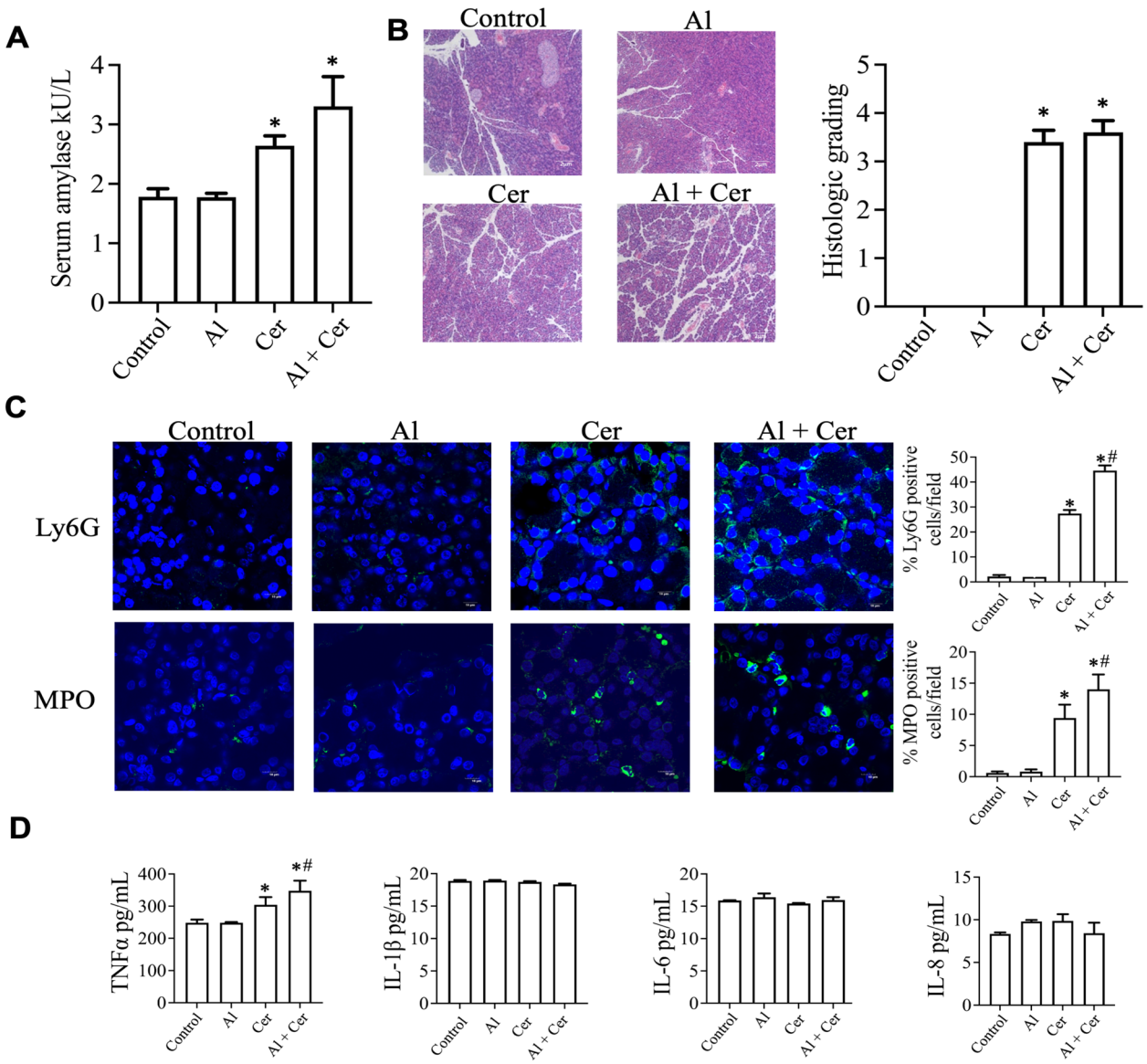

Fig. 1 Alcohol treatment aggravates the cerulein-induced AP in rats. **A** The serum amylase levels in the four groups of rats were measured. **B** Representative photographs (×200) of hematoxylin–eosin-stained histological sections and histological grades of pancreatic tissue from rats. **C** Representative immunofluorescence images of Ly6G and MPO in rat pancreatic tissue sections, and the numbers of Ly6G- and MPO-positive cells were quantitatively analyzed; scale bar: 10 μm. $n = 5$ rats/group; $n = 7$ to 9 fields. **D** The serum levels of TNFα and interleukins in the four groups were measured by ELISA; $n = 5$ rats/group, and 3 samples/rat. *Statistically significant differences among the four groups (ANOVA, $P < 0.05$), #Statistically significant differences between the Cer-treated group and Al + Cer-treated group (*t* test, $P < 0.05$). The data are presented as the mean ± SEM. *Al* alcohol, *Cer* cerulein

(See figure on next page.)

Fig. 2 Alcohol treatment significantly increases the expression of CPT1A in the pancreatic tissues of rats. **A** Proteomic data: organelle localization, enriched KEGG pathways, and target protein identification. **B** Volcano plot showing differentially expressed proteins in the Al-treated group versus the control group and the Al + Cer-treated group versus the Cer-treated group. **C** The fold change in protein levels in the Al-treated group versus the control group and the Al + Cer-treated group versus the Cer-treated group. **D** Representative immunofluorescence images of CPT1A in pancreatic tissue sections from rats in the four groups, and the number of CPT1A-positive cells was quantitatively analyzed; scale bar: 10 μm. $n = 5$ rats/group; $n = 7$ to 9 fields. **E** The expression of CPT1A in the pancreatic tissue of the model rats in the four groups was measured by western blotting, and the fluorescence intensity was quantitatively analyzed. The results were obtained from three separate experiments. *Statistically significant difference values (*t* test $P < 0.05$); $n = 5$ rats/group. The data are presented as the mean ± SEM. *Al* alcohol, *Cer* cerulein

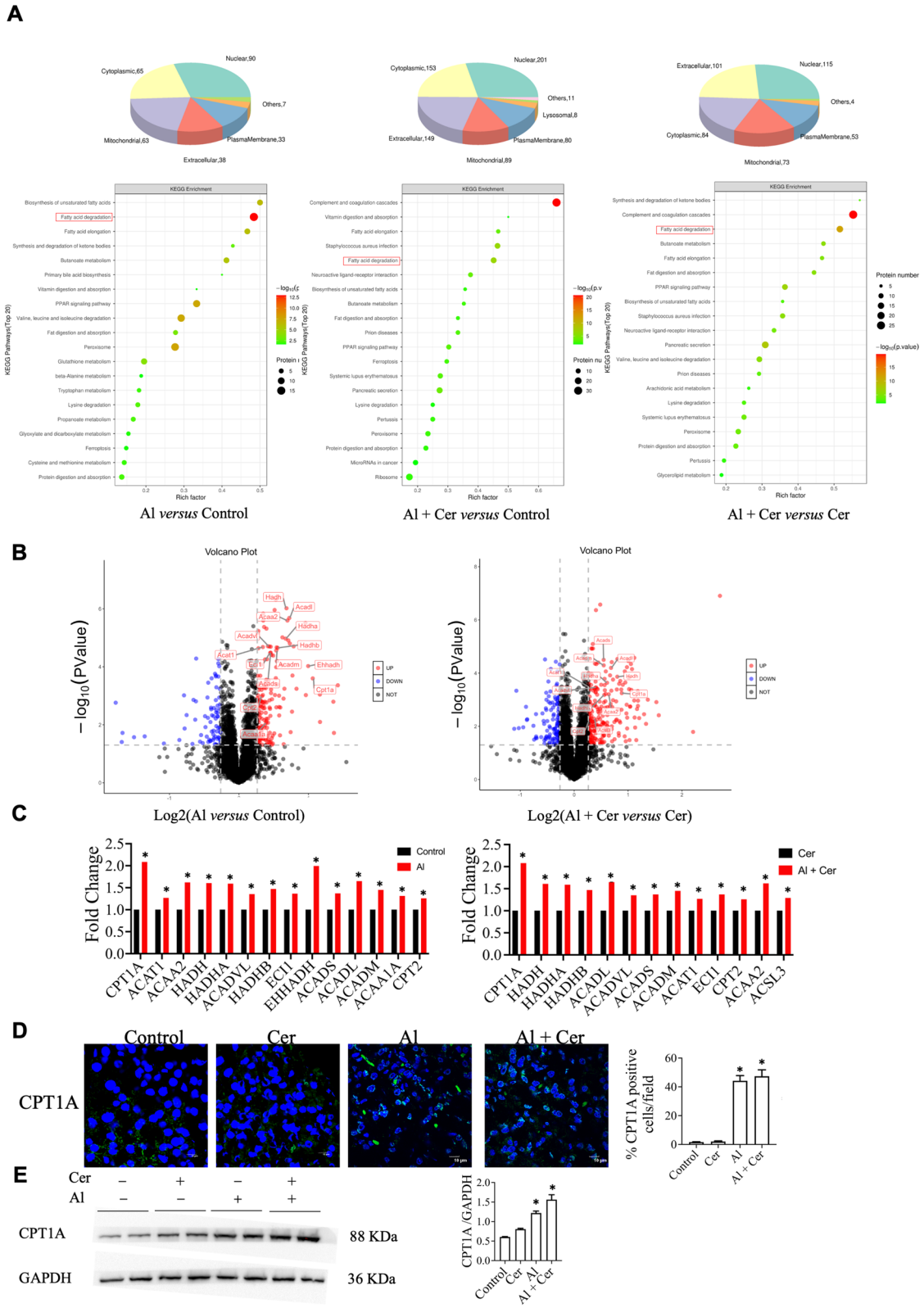

Fig. 2 (See legend on previous page.)

in the number of CPT1A-positive cells in the pancreatic tissue of the alcohol-treated rats and the AAP model rats, in contrast to the control group, and the WB results suggested increased CPT1A expression in the same case. All of these data revealed that alcohol may have contributed to the elevated expression of CPT1A in the pancreatic tissue of the rats (Fig. 2D).

Serum acylcarnitine levels are decreased in persons with a history of alcohol consumption

Metabolomic analyses of rat pancreatic tissue, rat serum and human serum revealed 34 classes of metabolites and a total of 377 species. A previous study showed that CPT1A catalyzed the formation of long-chain acylcarnitine from long-chain fatty acids and mediated the β-oxidation of fatty acids (FAO). First, the levels of acylcarnitines in the pancreatic tissue and serum of the rats were measured. The levels of short-chain acylcarnitines (isobutyryl-L-carnitine and isovaleryl-carnitine, c4 and c5) and medium-chain acylcarnitines (decanoyl-L-carnitine and decanoyl-carnitine, c8 and c10) were decreased significantly in the pancreatic tissue of alcohol-fed rats (Al) compared with the pancreatic tissue of control rats (Control), and there was an increase in the levels of long-chain carnitines (L-palmitoyl-carnitine and stearoyl-carnitine, c16 and c18). Thus, the pancreatic tissue of Al-treated rats had less accumulation of short- and medium-chain acylcarnitines and greater accumulation of long-chain acylcarnitines (Fig. 4A–C). In the serum of rats, the levels of short- and long-chain acylcarnitines (myristoyl-L-carnitine, L-palmitoyl-carnitine and stearoyl-carnitine, c14, c16 and c18) underwent the same changes as those in the pancreatic tissue. In addition, the levels of medium-chain acylcarnitines (octanoylcarnitine and decanoylcarnitine, c8 and c10) were greater in the serum of Al-treated rats (Fig. 4D–F). To explore the relevance of serum acylcarnitines in humans, this study measured serum acylcarnitine levels in a cohort of 20 persons with a history of alcohol consumption (PHA) and 20 individuals with no history of alcohol consumption (control). Lower levels of short- and medium-chain acylcarnitines were detected in the serum of the PHA, and the levels of short-chain acylcarnitines were consistent with those in the pancreatic tissue; moreover, there was a decrease in the level of long-chain acylcarnitines (with no significant difference) (Fig. 4G–I), suggesting that the decrease in the serum short- and medium-chain acylcarnitine levels most likely reflected the high activity of CPT1A associated with PHA. Additionally, these findings revealed that DL-carnitine serum levels in the PHA cohort were almost identical to those in the control cohort (Fig. 4J).

Alcohol alters lipid composition in rat pancreatic tissue

The above data indicate that alcohol promotes FAO in rat pancreatic tissue by regulating CPT1A expression. As shown in Fig. 5A, the total lipid content increased significantly in alcohol-fed rat pancreatic tissue, and after inhibition of CPT1A activity, the total lipid content decreased. This study evaluated whether alcohol affects lipid metabolism in rat pancreatic tissue. Compared with those in control rats, alcohol treatment significantly altered the lipid composition (Fig. 5B), with significantly increased levels of phospholipids (PC, PE, and PIP3) (Fig. 5C, D), and these effects were improved after inhibition of CPT1A activity, suggesting that alcohol not only promotes FAO but also alters lipid metabolism in rat pancreatic tissue by regulating CPT1A expression.

Etomoxir ameliorates alcohol-induced ROS production and oxidative stress-related protein expression in AR42J cells

This study further investigated the impact of alcohol on AR42J cells. Alcohol at various concentrations (2.5, 5 and 10 μg/mL) was applied for 8 h to stimulate the AR42J cells. In AR42J cells exposed to alcohol, 2.5 μg/mL alcohol led to the most pronounced upregulation of CPT1A protein expression (Fig. 6A). Recent studies have suggested that CPT1A promotes ROS production [17, 18]. Figure 6B shows that the total intracellular production of ROS in the AR42J cells after alcohol treatment increased nearly fourfold in contrast to that in the control cells. Etomoxir treatment attenuated the increase in total intracellular ROS production induced by alcohol. Intracellular ROS are mainly generated in mitochondria; therefore, this study further explored the influence of alcohol on mitochondrial ROS through the MitoSOX probe. As shown in Fig. 6C, etomoxir treatment suppressed alcohol-induced mitochondrial ROS production. The impact of etomoxir on the expression of proteins associated with

(See figure on next page.)

Fig. 3 Schematic summary of the results of a proteomic analysis used to compare the effects of alcohol + cerulein versus those of cerulein in rats. The differentially expressed proteins are shown, with red indicating upregulation. *CPT* carnitine palmitoyltransferase, *ACSL3* acyl-CoA synthetase long-chain family member 3, *CoA* coenzyme A, *ACAD* acyl-CoA dehydrogenase, *HADH* hydroxyacyl-CoA dehydrogenase, *HADHA* hydroxyacyl-CoA dehydrogenase trifunctional multienzyme complex subunit alpha, *HADHB* hydroxyacyl-CoA dehydrogenase trifunctional multienzyme complex subunit beta, *ACAA2* acetyl-CoA acyltransferase 2, *ACAT1* acetyl-CoA acetyltransferase 1, *CACT* carnitine–acylcarnitine–translocase

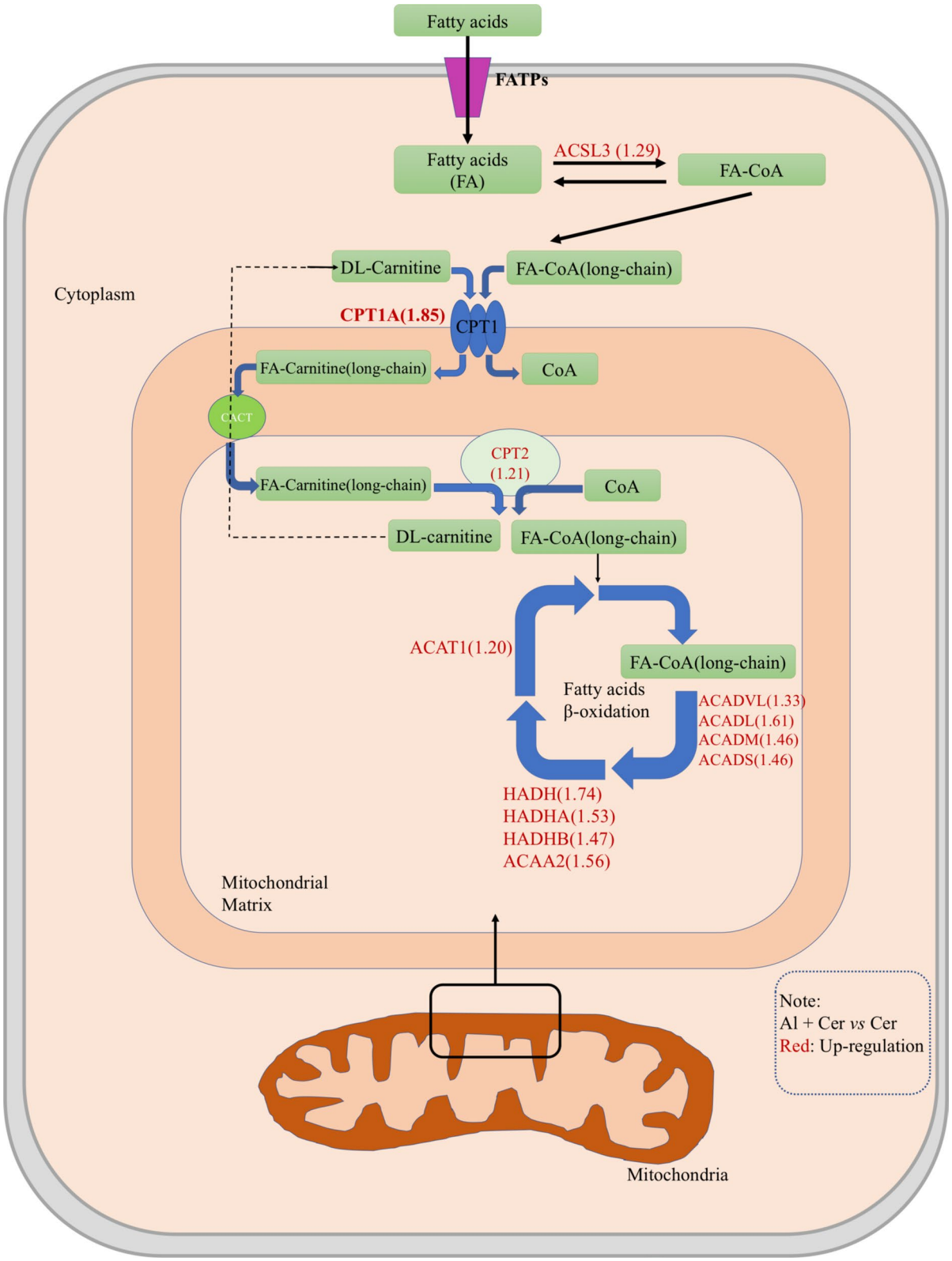

Fig. 3 (See legend on previous page.)

oxidative stress in AR42J cells treated with alcohol was further studied. The protein expression of GPX-1, CAT, and SOD1 in response to alcohol was markedly lower than that in the control group, and etomoxir reversed this phenomenon. However, alcohol exposure increased the protein expression of SOD2, which is a key antioxidant enzyme in the mitochondria. Etomoxir treatment reduced the alcohol-induced increase in the SOD2 protein level (Fig. 6D). These data suggested that inhibition of CPT1A activity protected the antioxidant defense system in AR42J cells treated with alcohol. In addition, Mito-TEMPO, a mitochondria-specific superoxide scavenger [19], alleviated the alcohol-induced increase in CPT1A expression (Fig. 6E). These results suggest that there is crosstalk between ROS and CPT1A in alcohol-treated AR42J cells.

Etomoxir attenuates mitochondrial dysfunction and accelerates the activity of amylase in alcohol-stimulated AR42J cells

Excessive mitochondrial ROS have been reported to cause mitochondrial dysfunction. Therefore, alterations in mitochondrial ultrastructure in the pancreatic tissue of rats were evaluated. Cerulein treatment did not significantly damage the mitochondrial ultrastructure of rat pancreatic tissue. In contrast, in alcohol-treated and AAP model rats, had fractured cristae and a subsequent reduction in crista bulk density, the number of mitochondrial elementary particles was reduced, and the electron density was decreased. Interestingly, alcohol- or alcohol + cerulein-induced mitochondrial ultrastructural damage was significantly ameliorated after etomoxir treatment in a rat model of pancreatitis (Fig. 7A).

To assess mitochondrial function, the fluorescent probe JC-1 was used to determine the MMP. Alcohol stimulation depolarized the mitochondrial membrane potential in the AR42J cells, as indicated by JC-1 changing from J-aggregates to monomers. Etomoxir intervention attenuated the MMP depolarization induced by alcohol (Fig. 7B). Next, this study attempted to determine the impact of alcohol stimulation on mitochondrial respiration in AR42J cells. In alcohol-stimulated AR42J cells, the OCR was detected by a Seahorse XFp Extracellular Flux Analyzer to assess mitochondrial respiration. As shown in Fig. 7C, alcohol stimulation led to mitochondrial stress in the AR42J cells, as evidenced by a significant decrease in the OCR. In alcohol-stimulated AR42J cells, the basal respiration rate, ATP production rate, MRR, and proton leakage of mitochondria were significantly lower than those in alcohol + etomoxir-treated cells, while the reserve capacity and the nonmitochondrial respiration rate were not significantly different (Fig. 7D). These data suggested that etomoxir mitigated alcohol-induced mitochondrial dysfunction in AR42J cells. Amylase activity in the intracellular and culture supernatants of alcohol-stimulated AR42J cells was also assayed (Fig. 7E). These results show that alcohol treatment results in reduced intracellular and extracellular amylase activity in AR42J cells. Etomoxir treatment restored amylase activity in response to alcohol. These data imply that inhibition of CPT1A activity protects the synthesis and secretion of amylase in alcohol-treated AR42J cells.

Inhibition of CPT1A activity attenuates inflammation in an AAP rat model

This research examined whether the suppression of CPT1A activity could mitigate AAP in a rat model. The number of CPT1A-positive cells was decreased in the pancreatic tissue of the AAP model rats subjected to etomoxir injection. DHE staining revealed reduced reactive oxygen species (ROS) levels in pancreatic tissue (Fig. 8A, B). Etomoxir treatment significantly decreased the serum IL-8 and TNF-α levels in the AAP rat model. Moreover, the infiltration of neutrophils (Ly6G- and MPO-positive cells) in pancreatic tissues was significantly reduced (Fig. 8C, D).

Discussion

Alcohol intake is thought to increase the sensitivity of the pancreas to the effects of other stressors, leading to disease [2]. However, when alcohol is combined with other risk factors, the inflammatory response is even greater, which is in line with earlier findings [20].

Several investigations have shown that the pancreas metabolizes alcohol primarily through fatty acid ethyl ester (FAEE) synthase, which produces FAEEs and has a toxic effect on PECs [5, 6]. Kaphalia et al. reported that [21] the expression of CPT1A was markedly reduced in PECs treated with 3 mg/mL and 6 mg/mL alcohol. However, alcohol levels of 3 mg/mL and 6 mg/mL are

(See figure on next page.)

Fig. 4 The levels of serum acylcarnitines are decreased in persons with a history of alcohol consumption (PHA). **A**–**C** Acylcarnitine (short-chain, medium-chain, and long-chain) levels in the pancreatic tissue of rats. **D**–**F** Acylcarnitine (short-chain, medium-chain, and long-chain) levels in the serum of rats; $n = 5$ rats/group. *Significant difference between the AI-treated group and the control group (*t* test, $P < 0.05$). **G**–**J** Acylcarnitine (short-chain, medium-chain, long-chain, and DL-carnitine) levels in the serum of humans. *Significant difference between the PHA and control cohorts (*t* test, $P < 0.05$). The results are presented as the mean ± SEM. *AI* alcohol, *PHA* persons with a history of alcohol consumption

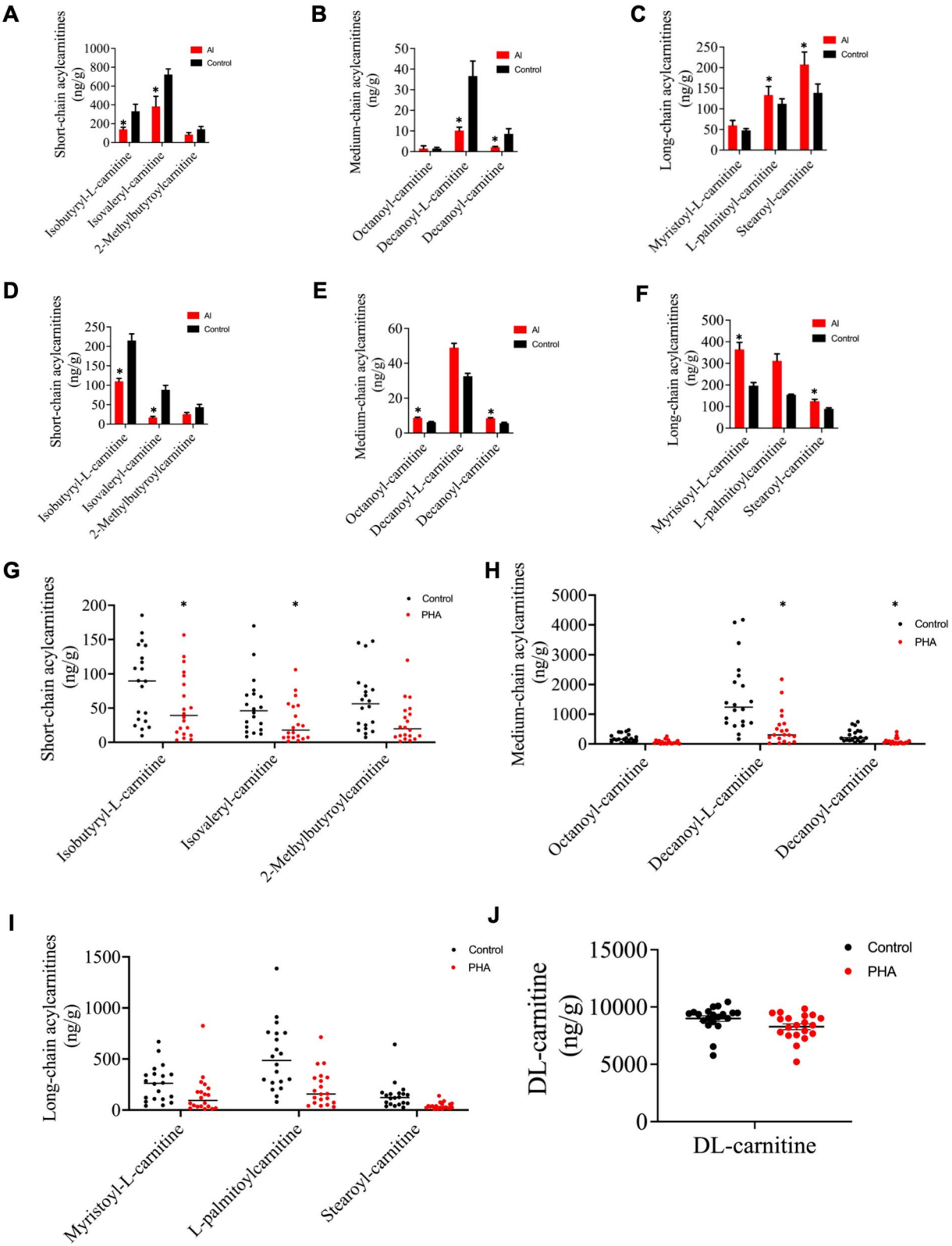

Fig. 4 (See legend on previous page.)

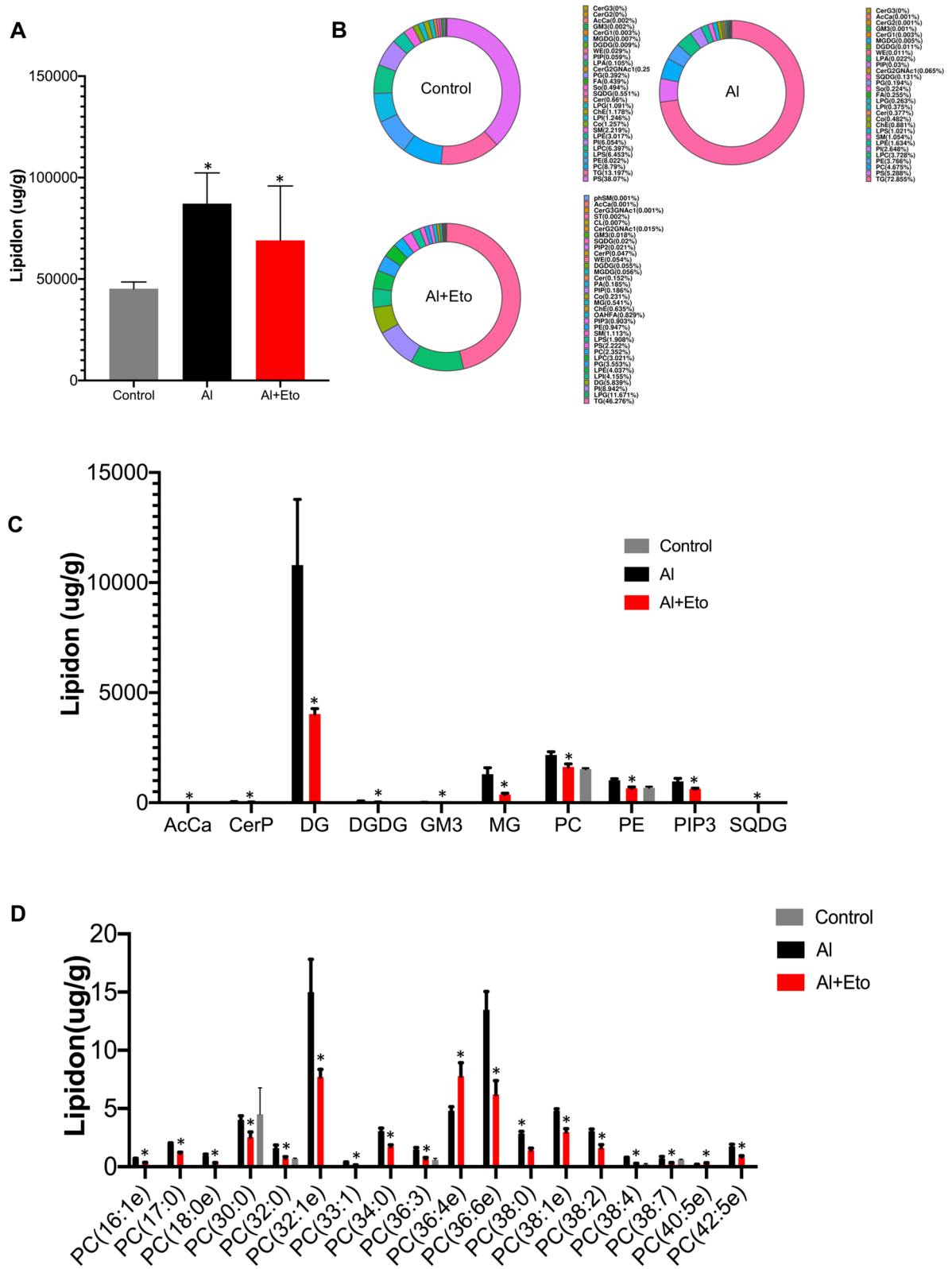

Fig. 5 Alcohol alters lipid composition in rat pancreatic tissue. **A** Total lipid content in rat pancreatic tissue. **B** Lipid composition in the pancreatic tissue of rats. **C**, **D** Part of lipid contents in pancreatic tissue from rats; $n = 5$ rats/group. *Significant difference between the AI-treated group and the AI + Eto-treated group (*t* test, $P < 0.05$). *AI* alcohol, *Eto* etomoxir

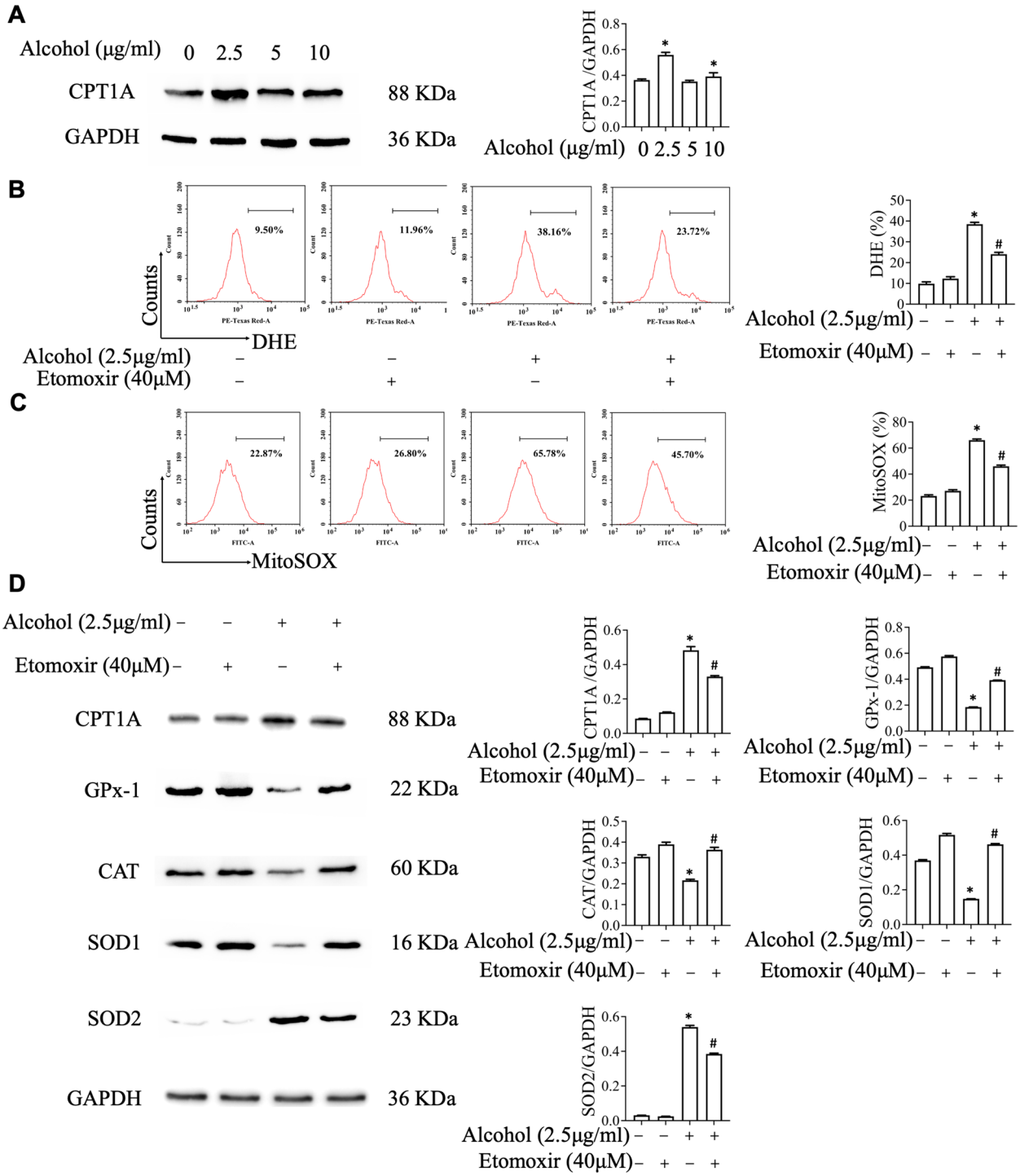

Fig. 6 Etomoxir ameliorates alcohol-induced ROS production and oxidative stress-related protein expression in AR42J cells. **A** The expression of CPT1A after treatment with different concentrations of alcohol (0 μg/mL, 2.5 μg/mL, 5 μg/mL, or 10 μg/mL) was determined by western blotting, and the fluorescence intensity was quantitatively analyzed. **B** The fluorescence intensity of DHE was measured via flow cytometry (FACS). **C** PECs were stained with MitoSOX, and the fluorescence intensity of MitoSOX was measured via FACS. **D** Changes in the expression of CPT1A, GPX-1, CAT, SOD1, and SOD2 after alcohol (2.5 μg/mL) stimulation with etomoxir (40 μM) or without etomoxir treatment were quantitatively analyzed. *Significant difference between the alcohol-treated group and the control group (*t* test, $P < 0.05$). #Significant difference after alcohol stimulation with and without etomoxir treatment (*t* test, $P < 0.05$). The results were obtained from three separate experiments and are presented as the mean ± SEM

well above the level of severe alcoholism, and a majority of patients with a history of alcohol consumption should have serum alcohol levels below this level. According to the proteomics results of this study, the expression of fatty acid degradation-related proteins in the pancreatic tissue of rats was significantly upregulated by alcohol intake. Long-chain acyl-CoA synthetases (ACSLs) are a family of enzymes that play an essential role in the metabolism of lipids via the conversion of free long-chain fatty acids to the acyl-CoA form [22]. Various ACSL isoforms partition fatty acids into particular cellular metabolic pathways, and fasting reduces ACSL5 and ACSL3 mRNA levels in the liver [23]. Importantly, the results of this study suggest that alcohol could upregulate ACSL3 in the pancreas. CPT1A is required for long-chain fatty acid transport to the inner mitochondrial membrane [24]. The carnitine acyl-carnitine translocase exchanges acyl-carnitine for DL-carnitine so that the cytosol does not become DL-carnitine depleted relative to the mitochondrion [24]. CPT2 on the inner side of the inner mitochondrial membrane transforms long-chain acylcarnitines into long-chain fatty acyl-CoA [24], thereby entering the fatty acid β-oxidation cycle. Among them, CPT1A was the most significantly altered enzyme in alcohol + cerulein-treated rat pancreatic tissue. This finding suggested that alcohol may regulate acute pancreatitis through FAO.

The inability to assess CPT1A levels in human pancreatic tissues presents limitations for a definitive interpretation. This study revealed a clear reduction in the serum levels of short- and medium-chain acylcarnitines in people who consumed alcohol, which was initially expected. The reduced short- and medium-chain acylcarnitine levels in the alcohol consumption cohort may be attributable to variations in CPT1A expression, as excessive shuttling of long-chain acylcarnitines may cause reduced accumulation of short- and medium-chain acylcarnitines [25] in an environment where there is no significant change in DL-carnitine levels. However, decreased long-chain acylcarnitine levels may result from an increased FAO rate. These results underscore the possible clinical relevance of a major FAO-related metabolic disruption in humans with a history of alcohol consumption.

Lipidomics was performed in this study and revealed that alcohol may regulate lipid metabolism in rat pancreatic tissue through CPT1A; in particular, the metabolism of phospholipids increased significantly in pancreatic tissue. Previous studies [22] have shown that ACSL4 is related to the metabolism of phospholipids, such as PC and PA, while this study revealed that CPT1A is related to the metabolism of phospholipids, especially PC, which may be associated with the modulation of FAO, mitochondrial respiration, and the formation of ATP by CPT1A, which affects the activity of ACSLs [26]. Among these phospholipids, phosphatidylcholine (PC) is the most abundant phospholipid in organelle membranes and eukaryotic cells [27], and other studies have shown that such lipid abnormalities may contribute to liver fibrosis and nonalcoholic steatohepatitis through the induction of inflammation, apoptosis, mitochondrial dysfunction, endoplasmic reticulum stress and oxidation [28]. These findings indicate that lipid metabolism plays an important role in regulating AAP.

ROS are intermediate products involved in redox reactions in aerobic metabolism [7]. Although ROS directly induce damage to pancreatic exocrine cells [8], this damage is seemingly not sufficient to cause AP. To explore the role of lipid metabolism-induced ROS production in AR42J cells, both intracellular and mitochondrial ROS production were evaluated. In the present study, alcohol-induced elevation of CPT1A expression in AR42J cells correlated with increased ROS levels. Mitochondrial ROS induce mitochondrial damage [8], and the mechanism is strongly associated with the loss of mitochondrial membrane potential [9]. This research demonstrated that alcohol treatment led to a dramatic decrease in the mitochondrial membrane potential in AR42J cells.

After etomoxir treatment, mitochondrial ultrastructure alterations were almost abrogated, which prevented the loss of intact mitochondrial cristae and led to an increase in the number of mitochondrial elementary

(See figure on next page.)

Fig. 7 Etomoxir attenuates mitochondrial dysfunction and accelerates the activity of amylase in alcohol-stimulated AR42J cells. **A** Representative electron microscopy images of PECs from rats in the control, Cer-treated, Al-treated, Al + Cer-treated, and Al + Cer + Eto-treated groups; $n = 5$ rats/group. **B** PECs were stained with JC-1, and the MMP was measured by FACS. *There were significant differences between the alcohol-stimulated group and the control group (*t* test, $P < 0.05$); #there was a significant difference between the groups treated without and with etomoxir (40 μM) after alcohol stimulation (2.5 μg/mL) (*t* test, $P < 0.05$). **C** Mitochondrial oxygen consumption was measured with a Seahorse XFp Extracellular Flux Analyzer. **D** Bar graph showing individual mitochondrial function parameters calculated from the data presented in **C**. *There was a significant difference between the groups with and without etomoxir treatment after alcohol stimulation (*t* test, $P < 0.05$). **E** The activity of amylase in intracellular and extracellular supernatants was determined by iodine–starch colorimetry. *Significant difference between the alcohol-treated group and the control group (*t* test, $P < 0.05$). #Significant difference groups with and without etomoxir treatment after alcohol stimulation (*t* test, $P < 0.05$). The results were obtained from three separate experiments and are presented as the mean ± SEM

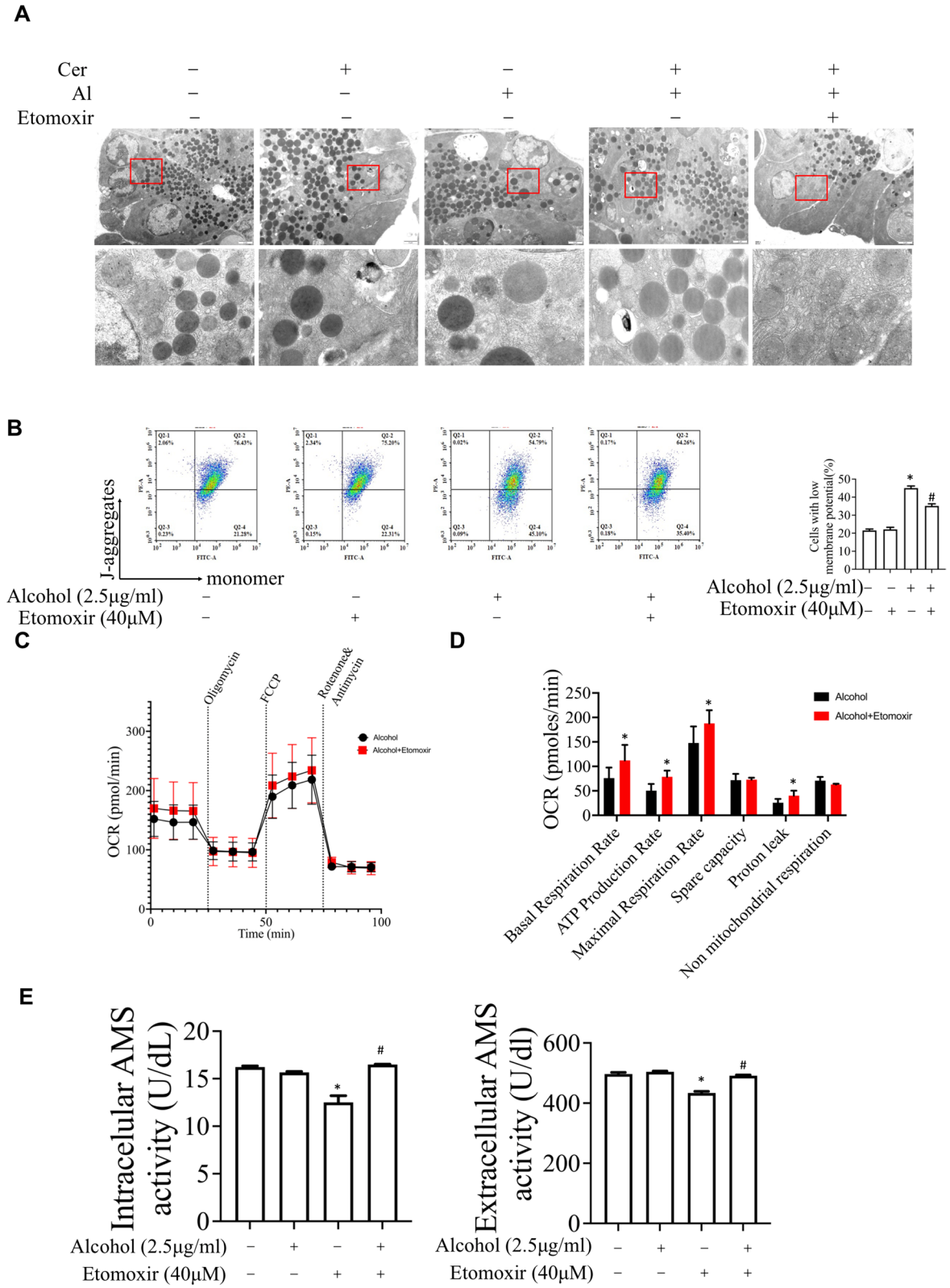

Fig. 7 (See legend on previous page.)

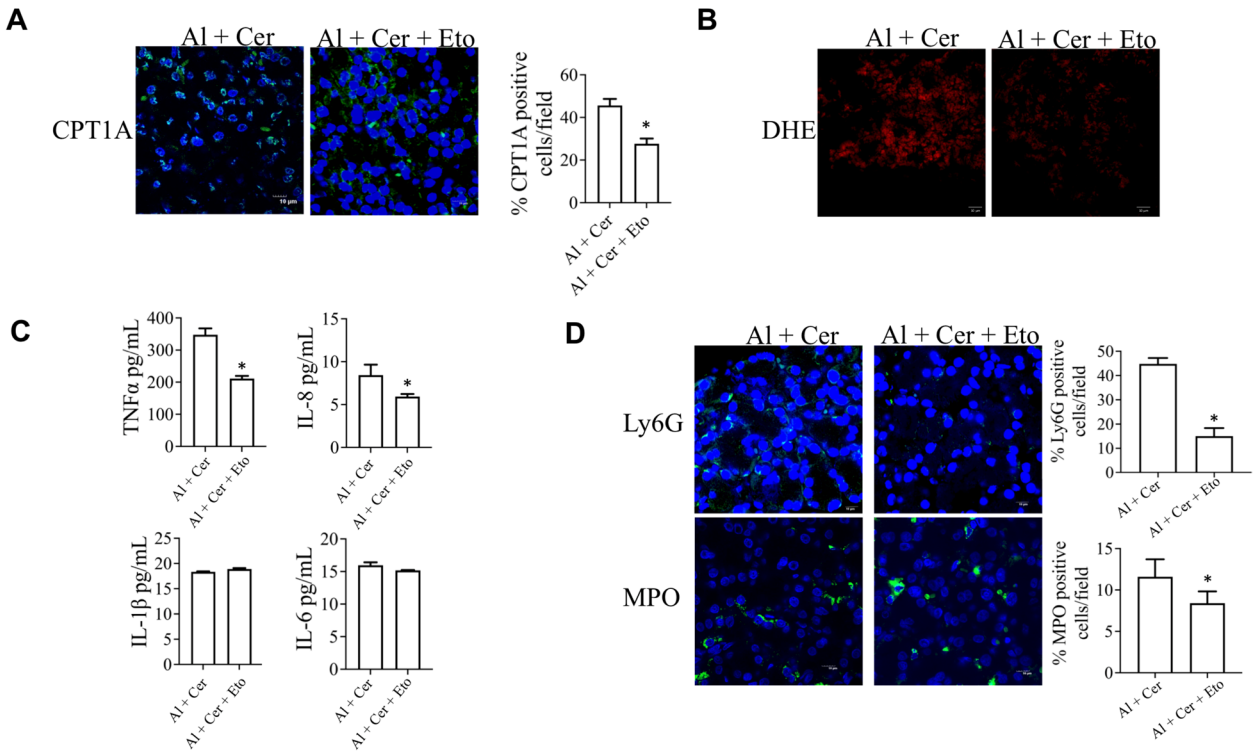

Fig. 8 Inhibition of CPT1A activity attenuates inflammation in an AAP rat model. **A** Representative immunofluorescence images of CPT1A in pancreatic tissue sections from Al + Cer-treated rats and Al + Cer + Eto-treated rats, and the number of CPT1A-positive cells was quantitatively analyzed; scale bar: 10 μm. $n = 5$ rats/group; $n = 7$ to 9 fields. **B** Representative DHE immunofluorescence images of pancreatic tissues from Al + Cer-treated rats and Al + Cer + Eto-treated rats; scale bar: 10 μm. $n = 4$ to 5 fields. **C** The serum levels of TNFα and interleukins in the Al + Cer-treated rats and Al + Cer + Eto-treated rats, as measured via ELISAs. **D** Representative immunofluorescence images of Ly6G and MPO in pancreatic tissue sections from Al + Cer-treated rats and Al + Cer + Eto-treated rats and the number of Ly6G- and MPO-positive cells were quantitatively analyzed; scale bar: 10 μm. $n = 5$ rats/group; $n = 7$ to 9 fields. *Significant difference between the Al + Cer-treated group and the Al + Cer + Eto-treated group (*t* test, $P < 0.05$). The results are presented as the mean ± SEM. *Al* alcohol, *Cer* cerulean, *Eto* etomoxir

particles. Folds in the inner mitochondrial membrane increase the surface area available for oxidative phosphorylation (OXPHOS) [29], and the elementary particles carry adenosine triphosphate (ATP) synthase, which uses energy produced by the respiratory chain to generate ATP. Furthermore, mitochondrial dysfunction was reversed to some extent after etomoxir treatment; specifically, etomoxir treatment improved the basal respiration rate, ATP production rate, MRR and proton leakage. These data revealed that etomoxir suppressed CPT1A expression in AR42J cells after alcohol stimulation and reduced mitochondrial dysfunction, suggesting that lipid metabolism, especially phospholipids metabolism, regulates pancreatic sensitization to necrosis and pancreatitis. Furthermore, this study explored the relationship between CPT1A activity and amylase activity in AR42J cells. Alcohol-treated AR42J cells displayed reduced intracellular and extracellular amylase activity, and etomoxir treatment increased amylase activity. These data imply that inhibition of CPT1A activity can improve the function of acinar cells.

The data in Fig. 1 suggest that alcohol alone causes minimal damage in the pancreas, but alcohol pretreatment exacerbates cerulein-induced AP in vivo models. Therefore, we further explore in vitro models how alcohol changes pancreatic cells before inflammation occurs. We treated AR42J cells with alcohol, and detected cellular and mitochondrial oxidative stress, mitochondrial morphology, oxidative respiration rate and other indicators. We found that although alcohol did not directly damage pancreatic cells, it affected some functions of the cells, which had a regulatory effect before the occurrence of inflammation, equivalent to a sentinel regulation.

Ahead findings have demonstrated that alcohol exerts various effects on pancreatic acinar cells by upregulating CPT1A expression, and these sentinel events act as a sentinel-regulation, although they do not directly cause acute pancreatitis. This study, through further controlled experiments, revealed that in an AAP rat model induced by alcohol + cerulein, preadministration of etomoxir prevented ROS production in pancreatic tissue and reduced the levels of TNFα and IL-8 in the serum. IL-8 recruits

neutrophils [30], which are landmark cells found in the early stage of AP [31]. Additionally, the number of MPO-positive cells and neutrophils was reduced in the etomoxir-pretreated AAP rats. This evidence, together with the reduction in the levels of TNFα and IL-8 in the serum, strongly suggested that inhibition of CPT1A alleviates the inflammatory response in alcohol-treated rats during AP.

Study strengths and limitations

Previous investigations have shown that pancreatic tissue metabolizes alcohol primarily through fatty acid ethyl ester synthase [5, 6]. According to the results of this study, alcohol also promotes the oxidation of fatty acids in pancreatic tissue by regulating CPT1A activity; this alters lipid metabolism, and the levels of phospholipids are significantly increased. Second, this study reveals for the first time that serum levels of short-chain and medium-chain acylcarnitines are reduced in persons with a history of alcohol consumption who are more prone to severe pancreatitis.

This study has several limitations. First, there are limitations in the measurement of CPT1A levels in human pancreatic tissue. CPT1A levels are currently reflected by acylcarnitine metabolism. In this study, the results of acylcarnitine metabolism in the pancreatic tissue of a rat model and in human serum were conjointly analyzed. Although the results for short-chain acylcarnitine were consistent, the link between pancreatic tissue and serum needs to be further investigated. This study demonstrated that etomoxir treatment can reduce the inflammatory response to AAP, but the effect of etomoxir on the liver was not considered in this study. In addition, in this study, several proteins were upregulated in alcohol-treated rats and downregulated after CPT1A inhibition, which are a family of fatty acid transporters, but no further localization experiments about these proteins have been conducted.

Conclusion

These findings suggest that alcohol is likely to regulate CPT1A-mediated lipid metabolism disorders that affect mitochondrial ultrastructure and function, which in turn sensitizes the pancreas to the impact of other stressors. Notably, the serum acylcarnitine results are clinically relevant, and the decrease in the serum levels of short- and medium-chain acylcarnitines in individuals that consume alcohol may reflect a greater susceptibility to severe AP.

Abbreviations

AP	Acute pancreatitis
AAP	Alcoholic acute pancreatitis
PECs	Pancreatic exocrine cells
CPT1A	Carnitine palmitoyl-transferase 1A
FAO	Fatty acid oxidation
IL-8	Interleukin-8
TNFα	Tumor necrosis factor α
DEPs	Differentially expressed proteins
LC–MS/MS	Liquid chromatography–tandem mass spectrometry
ROS	Reactive oxygen species
SOD	Superoxide dismutase
CAT	Catalase
GPX-1	Peroxidase-1
OCR	Oxygen consumption rate
MMP	Mitochondrial membrane potential
MPO	Myeloperoxidase
PHA	Persons with a history of alcohol consumption
IF	Immunofluorescence
HADH	Hydroxyacyl-CoA dehydrogenase
HADHA	Hydroxyacyl-CoA dehydrogenase trifunctional multienzyme complex subunit alpha
HADHB	Hydroxyacyl-CoA dehydrogenase trifunctional multienzyme complex subunit beta
ACADL	Acyl-CoA dehydrogenase, long chain
ACADVL	Acyl-CoA dehydrogenase, very long chain
ACADS	Acyl-CoA dehydrogenase short chain
ACADM	Acyl-CoA dehydrogenase medium chain
ACAT1	Acetyl-CoA acetyltransferase 1
ECI1	Enoyl-CoA delta isomerase 1
CPT2	Carnitine palmitoyltransferase 2
ACAA2	Acetyl-CoA acyltransferase 2
ACSL3	Acyl-CoA synthetase long-chain family member 3

Supplementary Information

The online version contains supplementary material available at https://doi.org/10.1186/s40001-024-02213-8.

Supplementary Material 1.

Acknowledgements

The authors were grateful to Metware Biotechnology Co., Ltd., for their contribution and assistance in lipidomics analysis.

Author contributions

All the authors contributed to the study conception and design. Material preparation, data collection and analysis were performed by Zenghui Li, Xinghui Li and Hui Jiang. The first draft of the manuscript was written by Zenghui Li, and all the authors commented on previous versions of the manuscript. All the authors have read and approved the final manuscript.

Funding

This work was supported by the National Natural Science Foundation of China (to XMZ, No. 81871440 and No. 82371961) and the Affiliated Hospital of North Sichuan Medical College (to XMZ, No. 2022JB001).

Data availability

No datasets were generated or analysed during the current study.

Declarations

Ethics approval and consent to participate

The Ethics approval and consent to participate was authorized by the Animal Bioethics Care Committee of North Sichuan Medical College (number 81871440).

Competing Interests

The authors declare no competing interests.

Author details

[1]Medical Imaging Key Laboratory of Sichuan Province, Department of Radiology, Affiliated Hospital of North Sichuan Medical College, 1# South Maoyuan Street, Nanchong 637001, Sichuan, China. [2] School of Basic Medical Sciences, Chengdu University of Traditional Chinese Medicine, 37# Shierqiao Road,

Chengdu 611137, Sichuan, China. [3]Department of Hepatobiliary Surgery, Affiliated Hospital of North Sichuan Medical College, 1# South Maoyuan Street, Nanchong 637001, Sichuan, China. [4]Department of General Surgery, Foshan Clinical Medical School of Guangzhou University of Chinese Medicine, 3# Sanyou South Road, Foshan 528000, Guangdong, China. [5]Department of Radiology, Ruijin Hospital, Shanghai Jiao Tong University School of Medicine, 197# Ruijin Er Road, Shanghai 200025, China. [6]Department of Pathology, Affiliated Hospital of North Sichuan Medical College, 1# South Maoyuan Street, Nanchong 637001, China. [7]Institute of Rheumatology and Immunology, Affiliated Hospital of North Sichuan Medical College, 63# Wenhua Road, Nanchong 637001, Sichuan, China.

Received: 14 April 2024 Accepted: 9 December 2024
Published online: 17 January 2025

References

1. Yadav D, Lowenfels AB. The epidemiology of pancreatitis and pancreatic cancer. Gastroenterology. 2013;144:1252–61.
2. Pandol SJ, Saluja AK, Imrie CW, Banks PA. Acute pancreatitis: bench to the bedside. Gastroenterology. 2007;132:1127–51.
3. Apte MV, Pirola RC, Wilson JS. Mechanisms of alcoholic pancreatitis. J Gastroenterol Hepatol. 2010;25:1816–26.
4. Shalbueva N, Mareninova OA, Gerloff A, Yuan J, Waldron RT, Pandol SJ, Gukovskaya AS. Effects of oxidative alcohol metabolism on the mitochondrial permeability transition pore and necrosis in a mouse model of alcoholic pancreatitis. Gastroenterology. 2013;144:437-446.e436.
5. Laposata EA, Lange LG. Presence of nonoxidative ethanol metabolism in human organs commonly damaged by ethanol abuse. Science. 1986;231:497–9.
6. Gukovskaya AS, Mouria M, Gukovsky I, Reyes CN, Kasho VN, Faller LD, Pandol SJ. Ethanol metabolism and transcription factor activation in pancreatic acinar cells in rats. Gastroenterology. 2002;122:106–18.
7. Parra-Robert M, Casals E, Massana N, Zeng M, Perramon M, Fernandez-Varo G, Morales-Ruiz M, Puntes V, Jimenez W, Casals G. Beyond the scavenging of reactive oxygen species (ROS): direct effect of cerium oxide nanoparticles in reducing fatty acids content in an in vitro model of hepatocellular steatosis. Biomolecules. 2019;9:425.
8. Criddle DN. Reactive oxygen species, Ca(2+) stores and acute pancreatitis; a step closer to therapy? Cell Calcium. 2016;60:180–9.
9. Lv L, Qin T, Huang Q, Jiang H, Chen F, Long F, Ren L, Liu J, Xie Y, Zeng M. Targeting tristetraprolin expression or functional activity regulates inflammatory response induced by MSU crystals. Front Immunol. 2021;12: 675534.
10. Lieber CS, DeCarli LM. The feeding of ethanol in liquid diets. Alcohol Clin Exp Res. 1986;10:550–3.
11. Fortunato F, Burgers H, Bergmann F, Rieger P, Buchler MW, Kroemer G, Werner J. Impaired autolysosome formation correlates with Lamp-2 depletion: role of apoptosis, autophagy, and necrosis in pancreatitis. Gastroenterology. 2009;137:350–60, 360.e351–5.
12. Kong L, Deng J, Zhou X, Cai B, Zhang B, Chen X, Chen Z, Wang W. Sitagliptin activates the p62-Keap1-Nrf2 signalling pathway to alleviate oxidative stress and excessive autophagy in severe acute pancreatitis-related acute lung injury. Cell Death Dis. 2021;12:928.
13. Luiken JJ, Niessen HE, Coort SL, Hoebers N, Coumans WA, Schwenk RW, Bonen A, Glatz JF. Etomoxir-induced partial carnitine palmitoyltransferase-I (CPT-I) inhibition in vivo does not alter cardiac long-chain fatty acid uptake and oxidation rates. Biochem J. 2009;419:447–55.
14. Song D, Zhou X, Yu Q, Li R, Dai Q, Zeng M. ML335 inhibits TWIK2 channel-mediated potassium efflux and attenuates mitochondrial damage in MSU crystal-induced inflammation. J Transl Med. 2024;22:785.
15. Gukovskaya AS, Gukovsky I, Zaninovic V, Song M, Sandoval D, Gukovsky S, Pandol SJ. Pancreatic acinar cells produce, release, and respond to tumor necrosis factor-alpha. Role in regulating cell death and pancreatitis. J Clin Invest. 1997;100:1853–62.
16. Sinclair G, Collins S, Arbour L, Vallance H. The p.P479L variant in CPT1A is associated with infectious disease in a BC First Nation. Paediatr Child Health. 2019;24:e111–5.
17. Luo X, Sun D, Wang Y, Zhang F, Wang Y. Cpt1a promoted ROS-induced oxidative stress and inflammation in liver injury via the Nrf2/HO-1 and NLRP3 inflammasome signaling pathway. Can J Physiol Pharmacol. 2021;99:468–77.
18. Wang M, Wang K, Liao X, Hu H, Chen L, Meng L, Gao W, Li Q. Carnitine palmitoyltransferase system: a new target for anti-inflammatory and anticancer therapy? Front Pharmacol. 2021;12: 760581.
19. London A, Cohen M, Schwartz M. Microglia and monocyte-derived macrophages: functionally distinct populations that act in concert in CNS plasticity and repair. Front Cell Neurosci. 2013;7:34.
20. Pandol SJ, Periskic S, Gukovsky I, Zaninovic V, Jung Y, Zong Y, Solomon TE, Gukovskaya AS, Tsukamoto H. Ethanol diet increases the sensitivity of rats to pancreatitis induced by cholecystokinin octapeptide. Gastroenterology. 1999;117:706–16.
21. Srinivasan MP, Bhopale KK, Caracheo AA, Amer SM, Khan S, Kaphalia L, Loganathan G, Balamurugan AN, Kaphalia BS. Activation of AMP-activated protein kinase attenuates ethanol-induced ER/oxidative stress and lipid phenotype in human pancreatic acinar cells. Biochem Pharmacol. 2020;180: 114174.
22. Zhou X, Zhao R, Lv M, Xu X, Liu W, Li X, Gao Y, Zhao Z, Zhang Z, Li Y, et al. ACSL4 promotes microglia-mediated neuroinflammation by regulating lipid metabolism and VGLL4 expression. Brain Behav Immun. 2023;109:331–43.
23. Mashek DG, Li LO, Coleman RA. Rat long-chain acyl-CoA synthetase mRNA, protein, and activity vary in tissue distribution and in response to diet. J Lipid Res. 2006;47:2004–10.
24. Bartlett K, Eaton S. Mitochondrial beta-oxidation. Eur J Biochem. 2004;271:462–9.
25. Adams SH, Hoppel CL, Lok KH, Zhao L, Wong SW, Minkler PE, Hwang DH, Newman JW, Garvey WT. Plasma acylcarnitine profiles suggest incomplete long-chain fatty acid beta-oxidation and altered tricarboxylic acid cycle activity in type 2 diabetic African-American women. J Nutr. 2009;139:1073–81.
26. Ma Y, Zha J, Yang X, Li Q, Zhang Q, Yin A, Beharry Z, Huang H, Huang J, Bartlett M, et al. Long-chain fatty acyl-CoA synthetase 1 promotes prostate cancer progression by elevation of lipogenesis and fatty acid beta-oxidation. Oncogene. 2021;40:1806–20.
27. Wang L, Zhou M. Structure of a eukaryotic cholinephosphotransferase-1 reveals mechanisms of substrate recognition and catalysis. Nat Commun. 2023;14:2753.
28. Béland-Bonenfant S, Rouland A, Petit J, Vergès B. Concise review of lipidomics in nonalcoholic fatty liver disease. Diabetes Metab. 2023;49: 101432.
29. McWherter C, Choi YJ, Serrano RL, Mahata SK, Terkeltaub R, Liu-Bryan R. Arhalofenate acid inhibits monosodium urate crystal-induced inflammatory responses through activation of AMP-activated protein kinase (AMPK) signaling. Arthritis Res Ther. 2018;20:204.
30. Luster AD. Chemokines–chemotactic cytokines that mediate inflammation. N Engl J Med. 1998;338:436–45.
31. Chooklin S, Pereyaslov A, Bihalskyy I. Pathogenic role of myeloperoxidase in acute pancreatitis. Hepatobiliary Pancreat Dis Int. 2009;8:627–31.

Publisher's Note